# TCSC CONTROLS FOR LINE POWER SCHEDULING AND SYSTEM OSCILLATION DAMPING – RESULTS FOR A SMALL EXAMPLE SYSTEM

Nelson Martins          Herminio J.C.P. Pinto
CEPEL
P.O. Box 68007
21944-970 – Rio de Janeiro – RJ – BRAZIL
pacdyn@fund.cepel.br

John J. Paserba
Mitsubishi Electric Power Products, Inc.
512 Keystone Drive
Warrendale, PA  15086 USA
john.paserba@meppi.mea.com

*Abstract* – This paper describes, in a tutorial manner, TCSC control aspects illustrated through simulation results on a small power system benchmark model. The analysis and design of the TCSC controls, to schedule line power and damp system oscillations, are based on modal analysis, and time and frequency response techniques. Root-locus plots are also utilized. The impact of badly located zeros on the system transient response is assessed and possible solutions are proposed. The data used for the power system model is provided so that others may duplicate or expand the results presented here.

*Keywords* – FACTS Controllers, Eigenanalysis, Controller Design, System Oscillations

## 1. INTRODUCTION

The potential benefits of Flexible AC Transmission Systems (FACTS) are now widely recognized by the power system engineering community [1,2]. Two Thyristor Controlled Series Compensation devices (TCSC), the first of a new generation of FACTS controllers [3,4], are already commissioned along with a Thyristor Switched Series Capacitor (TSSC), all in North America [5]. There are two other TCSCs to be commissioned in early 1999 in South America [6]. The short-term need to assess the impact of FACTS technology has led to R&D efforts on modeling, methodologies and software for static and dynamic analyses, and control strategies. Dynamic studies must contemplate both low and high frequency phenomena, calling for the use of different computer tools.

This paper deals with small-signal electromechanical stability, focusing attention on TCSC control aspects. A tutorial exercise on TCSC oscillation damping control and line power scheduling strategies is presented using a small power system benchmark model. A control structure is proposed for the practical implementation of the "constant angle" strategy. This strategy was devised in [8] to allow the rerouting of incremental power transfers in interconnected power systems. Eigenvalue, frequency and step response results are provided. Root-loci of power system transfer function poles are included. The impact of badly located zeros on the system transient response is assessed and shown to be minimized by proper choice of the TCSC stabilizing signal. Non-linear time domain simulations were not considered here. However, for a complete control study, it is prudent to use non-linear time domain simulations (including device limits) to verify the small-signal results. Full data on the example power system utilized are provided in the Appendix so the results may be reproduced or expanded upon by others.

## 2. TCSC CONTROLS AND POWER SYSTEM MODEL DESCRIPTION

The example system model (see Fig. 1 and Appendix) comprises a salient-pole synchronous generator connected to an infinite bus through a step-up transformer followed by two transmission circuits. The three operating points considered correspond to generation levels of 500 and 1000 MW and include one line outage case.
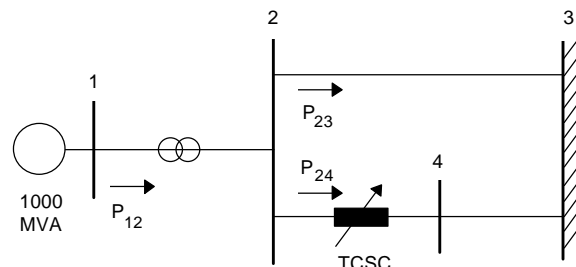


Fig. 1. Small Power System with TCSC.

The generator has a $5^{th}$ order model with data described in the Appendix. The automatic voltage regulator is represented by a first-order transfer function, also given in the Appendix. The TCSC device is located in line 2-4.

### 2.1 TCSC Model and Control System Diagram

Fig. 2 shows the control system diagram of a TCSC connected to a transmission line, considering the dynamics of the entire power system model. The blocks PI(s) and STAB(s) denote the transfer functions of the TCSC line scheduling controller and stabilizing signal, respectively. The blocks $F_1(s)$ and $F_2(s)$ relate the TCSC output (variable line series susceptance, $B_{2-4}$) to the controlled system variable ($x_{cont}$) and the variable used as the input to the stabilizer, ($x_{inp}$). Functions $F_1(s)$ and $F_2(s)$ have the same order as the number of system state variables. The symbol $x_{ref}$ denotes the TCSC reference or setpoint, whose value in steady-state is equal to $x_{cont}$.

The TCSC model consists of incremental current injections into the power system network at buses *2* and 4, which are assumed to be the device terminals. The initial value for its susceptance ($B_{2-4}^{0}$) is the line 2-4 series susceptance, which is directly modeled into the power flow equations. The incremental series susceptance ($\Delta B_{2-4}$) is determined, at any instant, by the output of the TCSC device. The TCSC stabilizer output is likewise modeled as a variable series susceptance ($\Delta B_{stab}$).
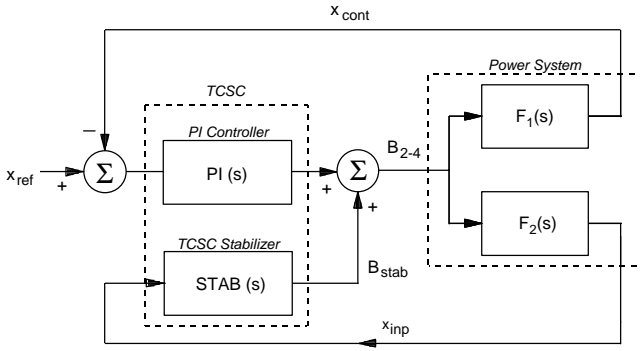
Fig 2. TCSC Control System Diagram.

**Note:** The symbol x, (e.g., $x_{ref}$ or $x_{inp}$) is used here to denote a generic system variable and does not necessarily refer to line reactance.

A more detailed block diagram of the TCSC Proportional-Integral (PI) controller and stabilizer is given in Fig. 3. The PI control action is quite slow in practice, since the line power scheduling is meant to be done over a period of about 20s. The parameters for the PI controller are given in Fig. 3. The parameters of the TCSC stabilizer differ according to its input variable, as shown in the following pages and figures of this paper. The TCSC stabilizer depicted in Fig. 3 has a block diagram similar to those used by generator exciter based power system stabilizers. The PI controller is meant for steady-state control, where the TCSC stabilizer is meant to provide rapid control, particularly for transient events.

The TCSC thyristor firing and other delays are usually represented by a single lag of 15ms, but were not modeled because they do not significantly impact the electromechanical stability phenomena [3,7].

### 2.2 TCSC Line Power Scheduling Strategies

Two strategies for scheduling the power flow of line 2-4 through the TCSC device were modeled by changing the $\Delta x_{cont}$ signal depicted in Figs. 2 and 3. One strategy keeps the power flow in line 2-4 at a specified value ($\Delta x_{cont} = \Delta P_{24}$) and will here be referred to as "constant line power" strategy. The other strategy is to make line 2-4 absorb any changes in generated power ($\Delta x_{cont} = \Delta P_{24} + \Delta P_{21}$). The latter is known as the "constant-angle" strategy [8] since it keeps the steady-state flows in parallel fixed impedance paths at constant level.
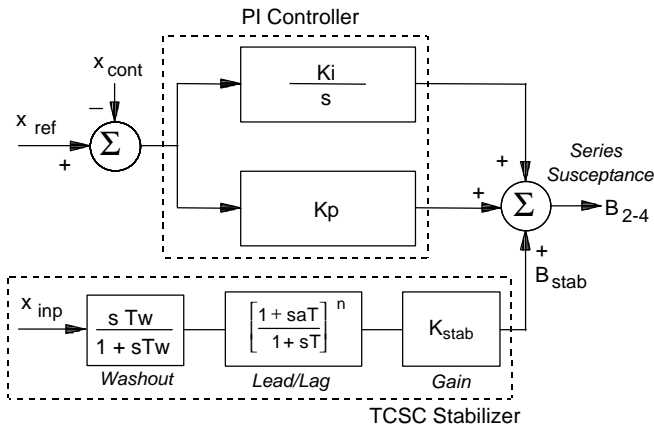


Ki = 10, Kp = 1 in all cases.

Fig 3. TCSC Controls.

The "constant angle" control structure proposed in this paper would require the telecommunication of the signal $\Delta P_{21}$, in the case it were remote, but this approach would still lead to a reliable and inexpensive practical implementation due to the slow dynamics of the line power scheduling process.

The "constant angle" control strategy can be synthesized through use of local signals only [8]. The approach is to develop angle difference across the system by synthesizing voltages behind reactances in both directions away from the TCSC based on local voltage and line current. This is illustrated in Fig. 4(a). However, care must be taken when developing the synthesizing parameters [9]. Another approach receiving recent attention is to directly measure phase-angle using synchronized phasor measurement units as illustrated in Fig. 4(b) [10].
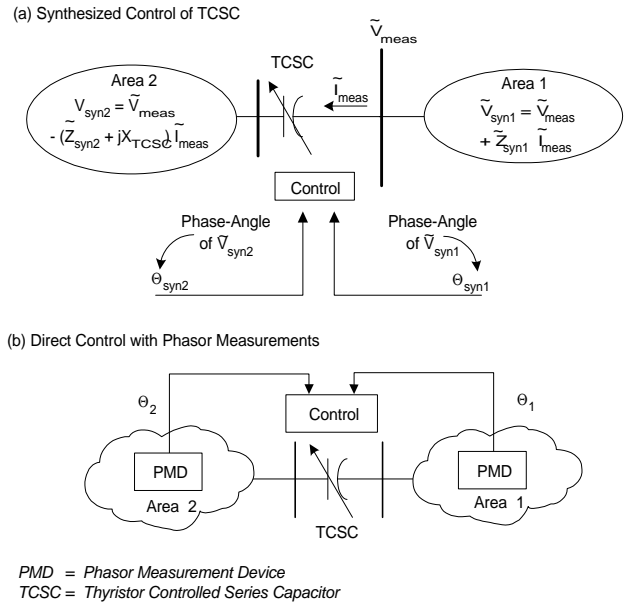


PMD = Phasor Measurement Device
TCSC = Thyristor Controlled Series Capacitor

Fig 4. Remote Voltage Phasors and Angle Difference using (a) Locally Measured Signals, (b) Direct Phasor Measurements.

### 3. POWER SCHEDULING RESULTS FOR A 500 MW TRANSFER

Table I displays the system eigenvalues for three different cases. Case A corresponds to the system with the TCSC operating at constant reactance mode. Note that in this operating mode, the TCSC controls depicted in Fig. 3 do not exist. Case B considers the presence of the TCSC at line 2-4 regulating its own power flow ("constant line power" control). Case C refers to the TCSC controls designed to make line 2-4 absorb all of the increased power flow in line 1-2 ("constant angle" control). This strategy is implemented in Case C by defining the variable $\Delta x_{cont} = \Delta P_{24} + \Delta P_{21}$. The TCSC does not have the damping control loop (TCSC stabilizer) in cases B and C.

Note from Table I that the electromechanical mode has approximately the same frequency ($\omega \approx 6.2$ rad/s) and damping in all cases, showing that the slowly acting line power scheduling control of the TCSC does not adversely impact the generator synchronizing and damping torques.

Table I. Eigenvalue Results for Cases A, B and C
(Generation Level of 500 MW)

| A | TCSC at Constant Reactance Mode | B | TCSC with Constant Line Power Controller |
|---|---|---|---|
| | -24.634 | | -24.636 |
| | -3.940 ± j6.901 | | -3.934 ± j6.894 |
| | -6.505 | | -6.507 |
| | -0.362 ± j6.219 | | -0.389 ± j6.203 |
| | | | -0.120 |
| C | TCSC with Constant Angle Controller | | |
| | -24.633 | | |
| | -3.946 ± j6.907 | | |
| | -6.503 | | |
| | -0.334 ± j6.235 | | |
| | -0.120 | | |

Step response results of the linearized system help to evaluate the performance of the two line power scheduling alternatives. The applied disturbance is a 1% step in the mechanical power of the synchronous generator ($\Delta P_{mec}$). The only exception is Fig. 12, whose plots relate to a step disturbance applied to the reference ($x_{ref}$) of the TCSC line power scheduling controller. The monitored variables are the active power flow deviations in the lines of the system ($\Delta P_{12}$, $\Delta P_{23}$, $\Delta P_{24}$ and $\Delta P_{43}$).

Figs. 5, 6 and 7 show the step responses for Cases A, B, and C, whose eigenvalues were displayed in Table I. The eigenvalues associated with the electromechanical oscillation, which are dominant in these responses, are also shown in the captions of these figures. Fig. 5 refers to Case A and shows that, in the absence of a TCSC device, the generated power step change $\Delta P_{12}$ is equally shared between the two circuits of the transmission corridor because the impedances of the two circuits are the same, as summarized in the Appendix. Case B results (Fig. 6) show the power flow in line 2-4 returning to its scheduled pre-disturbance value through TCSC action. The increased power transfer eventually flows solely through the parallel path (line 2-3).

Case C results (Fig. 7) show the compensated line 2-4 absorbing all of the increased active power generation. The power flow in the parallel path (line 2-3) is seen to settle down at the pre-disturbance value. Note that the electromechanical oscillations near 1 Hz (6.2 rad/s) die out
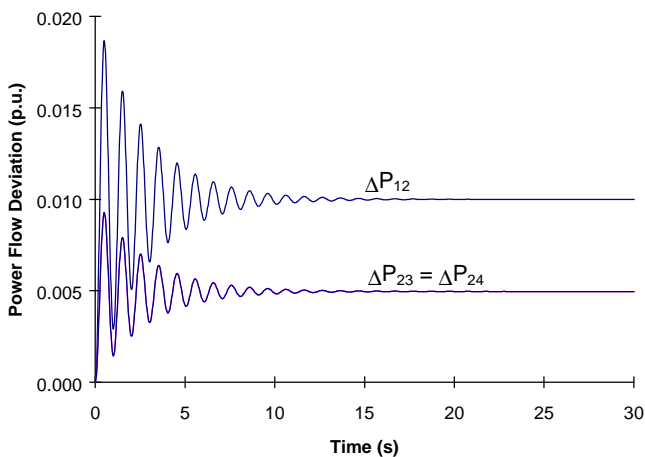


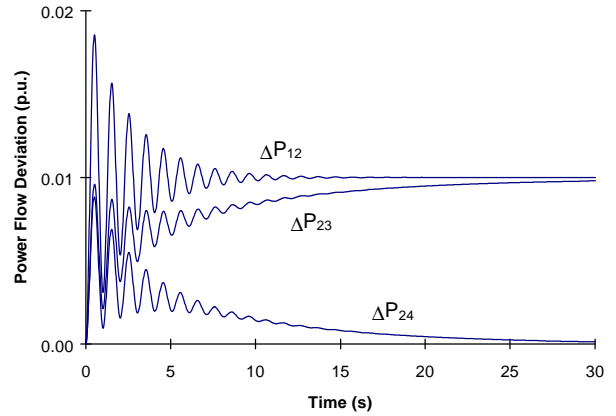Fig 5. Case A – System with TCSC at Constant Reactance Mode (dominant mode $\lambda = -0.362 \pm j6.219$).



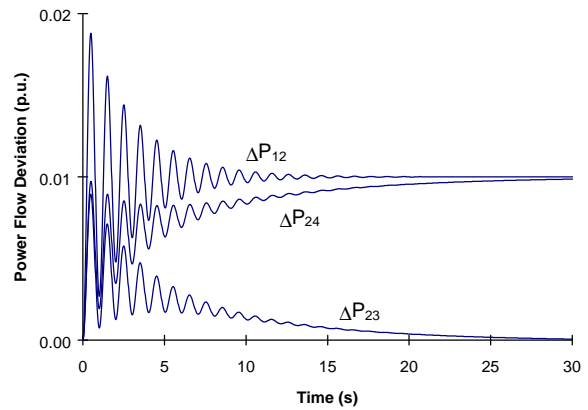Fig 6. Case B – TCSC with "Constant Line Power" Controller (dominant mode $\lambda = -0.389 \pm j6.203$).



Fig 7. Case C – TCSC with "Constant Angle" Controller (dominant mode $\lambda = -0.334 \pm j6.235$).

after about 10s. The response of the TCSC line power scheduling controller (Figs. 6 and 7) is slow and monotonic, being determined mostly by the real eigenvalue $\lambda = -0.12$.

The TCSC device was here seen to be very effective for line power scheduling, without causing adverse effects to power system oscillation damping. The next section describes the TCSC ability in providing additional damping to system oscillations through use of supplementary signals.

A controllable device must perform satisfactorily under all system conditions. TCSC controls, for example, must in practice be designed to also avoid potential control problems associated with line outage conditions, as described in Section 5.

## 4. OSCILLATION DAMPING CONTROL THROUGH TCSC STABILIZER ACTION

### 4.1 Damping Control [12]

Cases D, E and F refer to a system condition with a power transfer of 1000 MW, which is a transfer level where damping has long become a critical issue. The TCSC line power scheduling controls and parameters are the same as Case B, discussed in Section 3 (Constant Line Power Strategy). The electromechanical mode ($\lambda = +0.473 \pm j5.993$) is seen to be unstable for Case D, due to the higher power transfer (Table II).

Table II. Eigenvalues for Cases D, E and F
(Generation Level of 1000 MW)

| TCSC with "Constant Line Power" Controller | | | |
|---|---|---|---|
| **D** | **Without Stabilizer** | **E** | **TCSC with STAB$_1$ (derived from $\Delta\omega$)** |
| | -24.392 | | -24.150 |
| | -4.619 ± j6.819 | | -9.459 |
| | -7.146 | | -4.140 ± j5.383 |
| | **+0.473 ± j5.993** | | -6.612 |
| | -0.228 | | -1.136 ± j6.117 |
| | | | -0.366 |
| | | | -0.219 |
| **F** | **TCSC with STAB$_2$ (derived from $\Delta P_{21}$)** | | |
| | -24.415 | | |
| | -4.885 ± j6.362 | | |
| | -7.067 | | |
| | -0.593 ± j6.110 | | |
| | -2.167 ± j1.507 | | |
| | -0.326 | | |
| | -0.229 | | |

Stabilization could be effected by adding a power system stabilizer to the generator excitation system, but here only the TCSC controls will be considered. An additional signal to the TCSC device will therefore be designed to stabilize the system.

TCSC stabilizer design is here based on Nyquist plots of a chosen Open Loop Transfer Function (OLTF), considering the control diagram of Fig. 2. The OLTF used for the design of stabilizer STAB(s) is shown below:

$$\frac{x_{inp}(s)}{B_{stab}(s)} = \frac{F_2(s)}{1 + F_1(s) \cdot P\,I(s)}$$

Closed loop stability for the open-loop unstable system ($\lambda = +0.473 \pm j5.993$) is obtained by ensuring a counter-clockwise encirclement of the -1 point by the Nyquist plot of the OLTF after feedback compensation. The reader is referred to [11,13] for more information regarding the frequency response design methods of this paper.

Generator speed was initially chosen as the TCSC stabilizer input ($x_{inp} = \omega$). The Nyquist plot in Fig. 8(a) shows the rotor speed signal needs high amplification but minimum phase advance. This result is in agreement with



Fig 8(b). Nyquist Plot of the OLTF $\Delta\omega(s)/\Delta B_{stab}(s)$. STAB$_1$(s) (dominant mode $\lambda = +.473 \pm j5.993$).
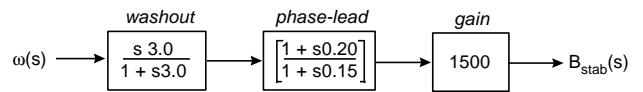


Fig 9. TCSC Stabilizer in Case E (STAB$_1$(s)).

current practice: using a proportional gain provides pure damping torque when the device input is speed or frequency and its output affects real power [8,9]. The feedback stabilizer function STAB$_1$(s) is designed to provide adequate gain and phase compensation to the rotor speed signal, as shown in Fig. 8(b), so as to achieve good closed loop performance.

The effectiveness of the stabilizer STAB$_1$(s) (Fig. 9) is verified from the eigenvalue results of Table II (Case E) and the step response plots of Fig. 10. The root locus plot for the electromechanical eigenvalue, as the TCSC stabilizer gain is varied, is pictured in Fig. 11. The minimum TCSC gain that turns the system stable is about 450, and no instability occurs for higher values of gain. The root locus results are in agreement with the gain margin information contained in the Nyquist plot of Fig. 8(b).

The system response (Case E) following a step disturbance in x$_{ref}$ is shown in Fig. 12. The TCSC controller correctly made line 2-4 to pick up more power at a very
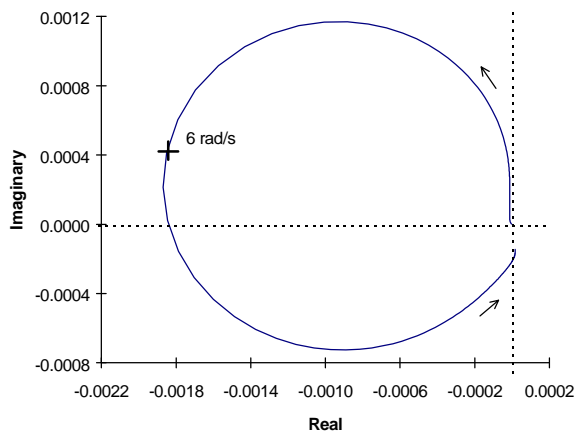


Fig 8(a). Nyquist Plot of OLTF $\Delta\omega(s)/\Delta B_{stab}(s)$ used for TCSC Stabilizer Design (dominant mode $\lambda = +.473 \pm j5.993$).
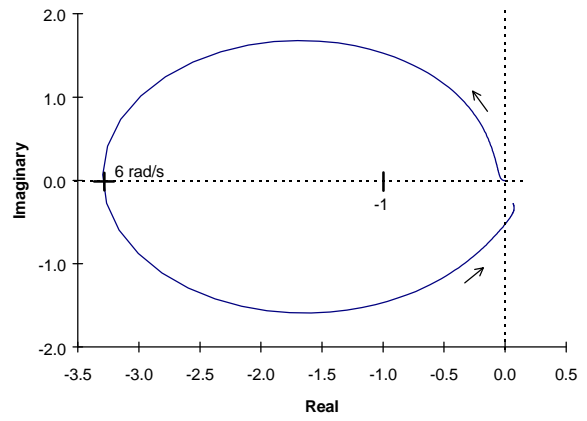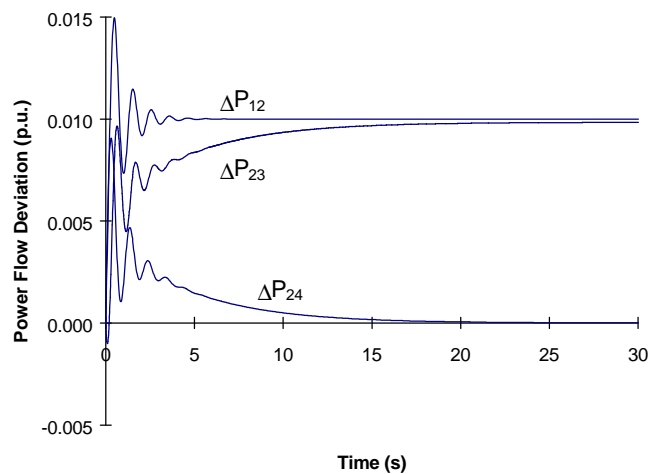


Fig 10. Case E – 1000 MW Transfer, TCSC Constant Line Power Control, STAB derived from $\Delta\omega$ (dominant mode $\lambda = -1.136 \pm j6.117$).

smooth rate, while line 2-3 had its power reduced accordingly. The active power deviations in line 1-2 are seen to return to zero after a minor transient.

The plots in Fig. 12 clearly show the benefits of designing a slowly acting TCSC line power scheduling controller: it causes very little impact on the electromechanical transients.
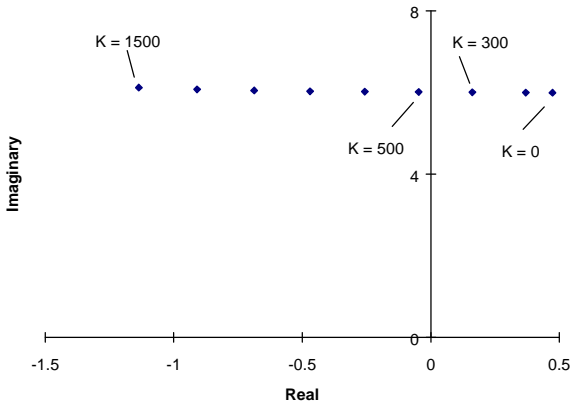


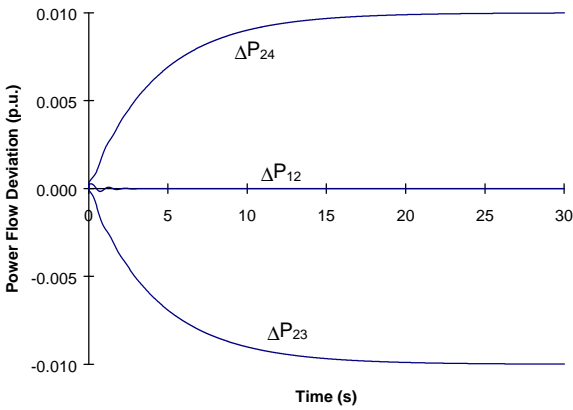Fig 11. Root Locus for Variable Gain in $STAB_1(s)$. Case E conditions are met for a gain value of 1500.



Fig. 12. Case E – Step Disturbance in the TCSC Line Power Order ($\Delta x_{ref}$) (dominant mode $\lambda = -0.219$).

## 4.2 Impact of Transfer Function Zeros on Transient Response

Badly located zeros can impair system stabilization, as described in [11,13]. They may also cause excessively high peaks in the transient response, despite the adequate damping of the system dominant poles. The latter effect can be seen in the example of this section (Case F).

The use of generator speed as the TCSC stabilizer input, is assumed to require signal telecommunication. To reduce cost and improve reliability, a local signal is always preferred. Assuming the TCSC to be located close to bus 2, implies that $P_{21}$ is a local signal, whose adequacy as the alternate stabilizer input is now assessed.

The analysis of Fig. 13(a) shows that the stabilizer derived for $\Delta P_{21}$ ($STAB_2(s)$) must provide considerable amplification and phase compensation: a lag of 85° is required at the center frequency of 6 rad/s. Fig. 13(b) shows the Nyquist diagram of the properly compensated system, which now has good phase and gain margins.
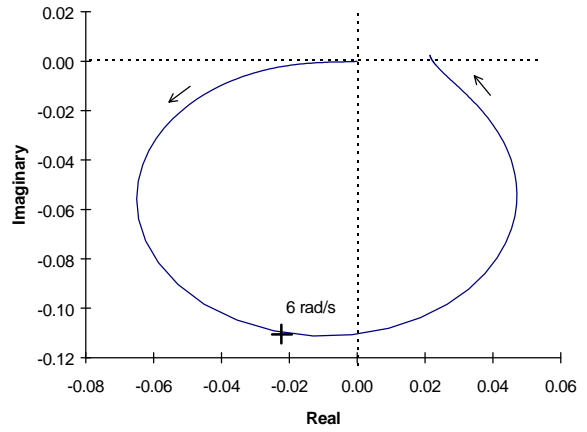


Fig 13(a). Nyquist Plot of OLTF $\Delta P_{21}(s)/\Delta B_{stab}(s)$ used for TCSC Stabilizer Design (dominant mode $\lambda = +.473 \pm j5.993$).
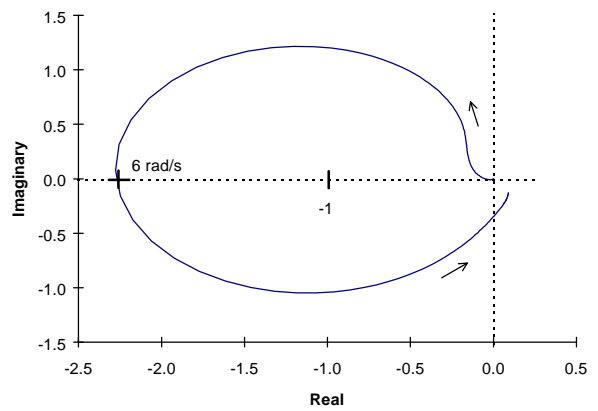


Fig 13(b). Nyquist Plot of the OLTF $(\Delta P_{21}(s)/\Delta B_{stab}(s)) \cdot STAB_2(s)$ (dominant mode $\lambda = +.473 \pm j5.993$).

As many readers may not be accustomed to Nyquist plots, the determination of gain margins, in association with Fig. 13(b), is briefly described here. Note that the OLTF $(P_{21}(s)/B_{stab}(s)) \cdot STAB_2(s)$ is linear with respect to the gain in $STAB_2(s)$. The Nyquist plot varies linearly with the gain of $STAB_2(s)$, and Fig. 13(b) was obtained for a gain of 100. For closed loop stability, the Nyquist plot must involve the -1 point in the counter-clockwise direction. Note that when the gain is reduced to 45, the system is on the verge of instability as the plot crosses the -1 point at a frequency of 6 rad/s. Note that the system again will be on the verge of instability for a gain of 2000, since the plot crosses the -1 point at a frequency of 1 rad/s. The Nyquist plot provides, therefore, information on the system conditional stability: ($45 < K_{TCSC} < 2000$). The same information is provided by the root locus plot in Fig. 16, where the critical gains and complex pole frequencies are displayed.

The eigenvalue and step response results for the Case F, with the TCSC stabilizer $STAB_2(s)$ derived from line 2-4 transit power were obtained (see Table II and Figs. 14 and 15).
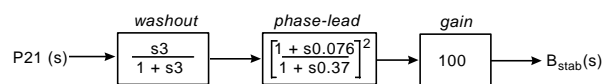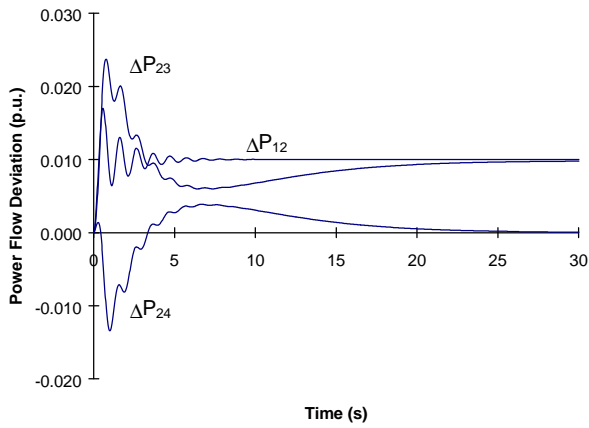


Fig. 14. TCSC Stabilizer in Case F ($STAB_2(s)$).

Fig 15. Case F – 1000 MW, TCSC Constant Line Power Control, STAB derived from $\Delta P_{21}$ (dominant mode $\lambda = -0.593 \pm j6.11$).

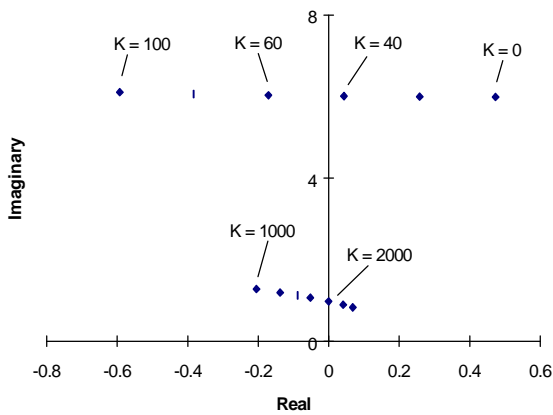

Fig 16. Root Locus Plot for Case F.

Fig. 15 shows there are excessively high peaks in the transient responses of $P_{23}$ and $P_{24}$. These high peaks are associated with the presence of zeros close to the origin for both the transfer functions $P_{23}/P_{mec}$ ($Z_{1,2} = 0.07 \pm j0.14$) and $P_{24}/P_{mec}$ ($Z = 0.09$). Note that the transfer function $P_{21}/P_{mec}$, which disregarding the minor resistive losses in the branch 1-2 is equal to the other two, does not present zeros close to the origin ($Z_1 = -0.23$ and $Z_2 = -0.33$) and consequently has adequate transient response.

Transfer functions $P_{23}/P_{mec}$ and $P_{24}/P_{mec}$ do not have zeros close to the origin when the TCSC stabilizer signal is derived from rotor speed ($Z_{1,2} = -0.37 \pm j0.033$). This desirable characteristic ranks rotor speed as a better signal than line transit power for TCSC damping control. An inferred signal that closely approximates the generator rotor speed can be synthesized from local signals only (voltage at bus 2 and current in line 1-2), as described in Section 2 and illustrated in Fig. 4. Assuming that the impedance of line 1-2 and the generator quadrature reactance are invariant or known at all times, the value for the internal generator quadrature voltage can be adequately inferred. The angle of this complex voltage ($\theta E_{qd}$), when processed by a derivative block, becomes equivalent to the generator rotor speed. The Bode diagrams for the transfer functions $\omega/B_{stab}$ and the derivative of $\theta E_{qd}/B_{stab}$ are compared in Fig. 17, and seen to
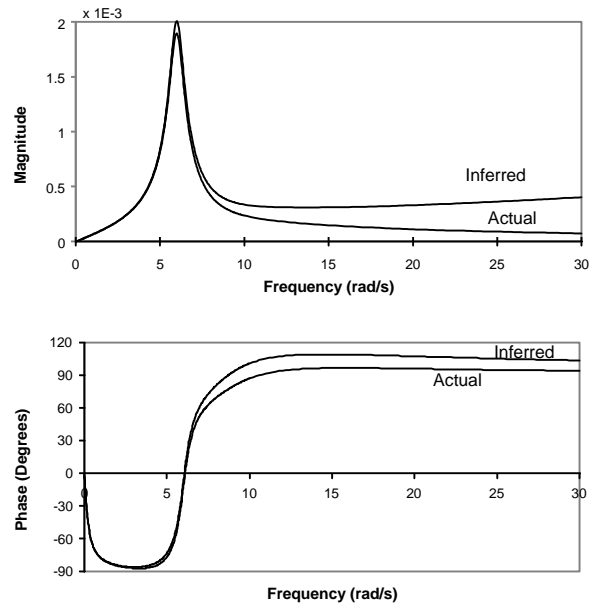


Fig 17. Frequency Responses for Actual and Inferred Rotor Speed.

be very similar. The inferred machine internal voltage is computed from the following expression:

$$E_{qd} = V_2 + j\left(X_{1-2} + X_q\right) \cdot I_{1-2}$$

Note that, as illustrated with the explanation on Nyquist plots previously in this section, that Bode techniques are often considered more practical for the analysis of large systems but Nyquist plots are more illustrative from the pedagogical point of view.

## 5. AVOIDING POTENTIAL PROBLEMS WITH TCSC CONTROLS DURING LINE OUTAGES

Case G, H and I refer to a 500 MW transfer during an outage of line 2-3. Case G refers to the system with the TCSC at constant reactance mode, which yields a highly oscillatory condition ($\lambda = -.044 \pm j5$). In Case H the TCSC has the constant line power controller and the stabilizer $STAB_1(s)$, as given in Fig. 9. Note that a zero eigenvalue appears in Case H (see Table III) indicating a complete lack of synchronizing torque at steady-state. This serious problem arises because the TCSC PI controller acts so as to eventually maintain constant power flow in line 2-4 irrespective of steady-state angle deviations at its terminals.

Table III. Eigenvalues for Cases H and I
Transfer of 500 MW Under Line Outage Condition

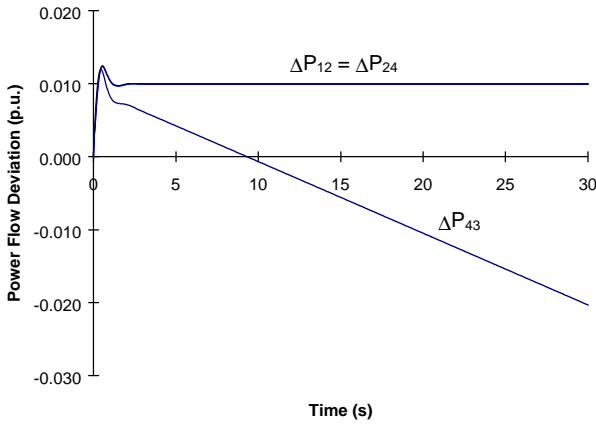| TCSC with Stabilizer $STAB_1(s)$ | | | |
|---|---|---|---|
| **H** | **With Constant Line Power Controller** | **I** | **Without Line Power Controller** |
| | -24.910 | | -24.896 |
| | -10.441 | | -10.449 |
| | -2.834 ± j7.623 | | -2.832 ± j7.590 |
| | -5.919 | | -5.917 |
| | -2.216 ± j3.393 | | -2.186 ± j3.505 |
| | -0.356 | | -0.356 |
| | 0.000 | | |

Fig 18. Case H – TCSC with "Constant Line Power" Controller for Line Outage Condition (dominant mode $\lambda = -2.216 \pm j3.393$; $\lambda = 0$).



Fig 19. Case I – TCSC Having Only Stabilizing Action During Line Outage Condition (dominant mode $\lambda = -2.186 \pm j3.505$).

It did not appear in Case B because line 2-3 was in-service and provided a free parallel path for synchronizing power exchanges between the generator and the infinite bus.

The linear step response results for Case H are displayed in Fig. 18, showing some serious control problems. The final value of the power change $\Delta P_{12}$ is equal to $\Delta P_{pref}$, the applied step disturbance to the generator mechanical power. The reference to the TCSC controller was left unchanged ($\Delta x_{ref} = 0$), and therefore a constant error is continuously seen by the PI controller. The susceptance $\Delta B_{24}$ will then decrease indefinitely, together with line current (until the TCSC limits are reached in the non-linear model). Fig. 18 shows that active power deviations $\Delta P_{43}$ decrease while $\Delta P_{24}$ settles at the same value as $\Delta P_{12}$. The drift associated with the zero eigenvalue would be avoided, if the same step disturbance were applied to both $P_{mec}$ and $x_{ref}$ inputs, but this is not a practical alternative.

The "constant line power" and "constant angle" strategies are meant to be applied to transmission systems having two or more parallel paths. The uncontrollable condition ($\lambda = 0$) observed in Case H eigensolution and time response results implies the system would remain drifting between the maximum and minimum output limits of the TCSC device. A special protection scheme would, therefore, be needed to inhibit the TCSC line power scheduling controls during some critical system contingencies. The TCSC damping function must however be left operational during such contingencies to keep the system damping at a satisfactory level.

Case I corresponds to the same line outage condition, but with the PI controller disconnected while maintaining the TCSC stabilizer loop operational. The eigenvalue results are also listed in Table III, showing the zero eigenvalue has disappeared.

The $STAB_1(s)$ transfer function was designed for another system condition (Case E) and has excessive gain for this case, yielding very large damping and a significant drop in frequency of the electromechanical mode ($\lambda = -2.186 \pm j3.505$). The step response results for Case I are shown in Fig. 19.
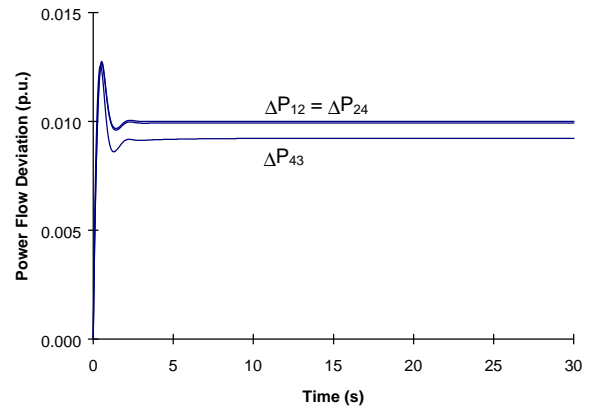
## 6. CONCLUSIONS

This paper presented, in a tutorial manner, the application of a TCSC for line power scheduling using both a constant power strategy and a constant angle strategy, and for damping electromechanical oscillations. A small benchmark power system model was used, with data provided so that others can reproduce or expand upon the results presented here. Several practical aspects of control design were illustrated including the potential problems of the TCSC control when parallel lines are outaged, and the impact of badly located zeros on the TCSC control. The results show the leverage of TCSC for power scheduling and for damping oscillations.

The results of this paper are clear examples of the benefits gained from the complementary use of modal analysis, frequency response and step response tools. The designed TCSC control and protection logic was seen to be robust, for the three operating conditions investigated, which included one line outage. Non-linear simulations confirmed this, but were not included in this paper due to space limitations.

## REFERENCES

[1] IEEE FACTS Working Group 15.05.15 in cooperation with CIGRE, "FACTS Overview," IEEE Special Publication 96-TP-108, 1996.

[2] Task Force on FACTS Applications of the IEEE FACTS Working Group 15.05.15 "FACTS Applications," IEEE Special Publication 96TP116-0, 1996.

[3] R.J. Piwko, C.A. Wegner, B.L. Damsky, B.C. Furumasu, J.D. Eden, "The Slatt Thyristor Controlled Series Capacitor Project-Design, Installation, Commissioning, and System Testing," CIGRE paper 14-104, Paris, 1994.

[4] N. Chistl, R. Hedin, K. Sadek, P. Lutzelberger, P.E. Krause, S.M. McKenna, A.H. Montoya, D. Torgerson, "Advanced Series Compensation (ASC) with Thyristor Controlled Impedance," CIGRE Paper 14/37/38-05, Paris, 1992.

[5] A.J.F. Keri, B.J. Ware R.A. Byron, M. Chamia, P. Halvarsson, L. Angquist, "Improving Transmission System Performance Using Controlled Series Capacitors," CIGRE Paper 14/37/38-07, Paris, 1992.

[6] C. Gama, R.L. Leoni, J.C. Salamao, J.B. Gribel, R. Fraga, M.J.X. Eiras, W. Ping, A. Ricardo, J. Cavalconti, "Brazilian North-South Interconnection – Application of Thyristor Controlled Series Compensation (TCSC) to Damp Inter-Area Oscillation Mode," SEPOPE Conference, Brazil, May 1998.

[7] S. Nyati, C.A. Wegner, R.W. Delmerico, D.H. Baker, R.J. Piwko, A. Edris, "Effectiveness of Thyristor Controlled Series Capacitor in Enhancing Power System Dynamics: An Analog Simulator Study," IEEE Transactions on Power Delivery, April, 1994, pp. 1018-1027.

[8] E.V. Larsen, C.E.J. Bowler, B. Damsky, S. Nilsson, "Benefits of Thyristor Controlled Series Compensation," CIGRE Paper 14/37/38-04, Paris, 1992.

[9] E.V. Larsen, J.J. Sanchez-Gasca, J.H. Chow, "Concepts for Design of FACTS Controllers to Damp Power Swings," IEEE Transactions on Power Systems, Vol. 10, No. 2, May 1995, pp. 948-956.

[10] EPRI WO3789-05, "Assessment of Applications and Benefits of Phasor Measurement Technology in Power Systems," Final Report by General Electric, EPRI Report TR-107903, April 1997.

[11] N. Martins and L.T.G. Lima, "Eigenvalue and Frequency Domain Analysis of Small-Signal Electromechanical Stability Problems," IEEE Symposium on Application of Eigenanalysis and Frequency Domain Methods for System Dynamic Performance, Special Publication 90TH0292-3PWR, pp. 17-33, 1990.

[12] CIGRE Task Force 38.01.07, "Analysis and Control of Power System Oscillations," CIGRE Technical Brochure No. 111, December 1996

[13] N. Martins, H.J.C.P. Pinto and L.T.G. Lima, "Efficient Methods for Finding Transfer Function Zeros of Power Systems," IEEE Transactions on Power Systems, Vol. 7, No. 3, pp. 1350-1361, August 1992.

## BIOGRAPHIES

**Nelson Martins** B.Sc. (72) Elec. Eng. from Univ. Brasilia, Brazil; M.Sc. (74) and Ph.D. (78) degrees from UMIST, UK. Dr. Martins has worked in CEPEL since 1978. He is the Chairman of CIGRE Task Force 38.02.16 on the Impact of the Interaction Among Power System Controls and has contributed to several IEEE Working Groups.

**Herminio J.C.P. Pinto** B.Sc. (86) and M.Sc. (90) Elec. Eng. from Fed. Univ. of Rio de Janeiro, Brazil. Since 1986 he has been with CEPEL and his current work and interests include power system operation and control and parallel processing.

**John J. Paserba** BEE (87) from Gannon University, Erie, PA., ME (88) from RPI, Troy, NY. Mr. Paserba worked in GE's Power Systems Energy Consulting Department for over 10 years before joining Mitsubishi Electric in 1998. He was the Chairman of CIGRE Task Force 38.01.07 on Control of Power System Oscillations, and has contributed to several IEEE Working Groups, Task Forces, and Subcommittees.

## APPENDIX

A.1 Example System Data

Frequency: 60 Hz
System and Generator Base: 1000 MVA for all cases.

Branch Data for All Cases

| Branch | | Impedance (%) | |
|---|---|---|---|
| From | To | R | X |
| 1 | 2 | 0.7 | 10. |
| 2 | 3 | 6.3 | 90. |
| 2 | 4 | 2.1 | 30. |
| 4 | 3 | 4.2 | 60. |

Note that line 2-3 is out-of-service in Cases G, H and I and that line 2-4 includes the combination of the line reactance and the TCSC reactance.

Bus Data for 500 MW Transfer

| Bus | $|V|$ pu | $\theta$ degrees | $P_{gen}$ MW | $Q_{gen}$ Mvar |
|---|---|---|---|---|
| 1 | 1.000 | 15.9 | 500. | 34.0 |
| 2 | 0.994 | 13.0 | | |
| 3 | 1.000 | 0.0 | -490.2 | 104.2 |
| 4 | 0.980 | 8.6 | | |

Bus Data for 1000 MW Transfer

| Bus | $|V|$ pu | $\theta$ degrees | $P_{gen}$ MW | $Q_{gen}$ Mvar |
|---|---|---|---|---|
| 1 | 1.000 | 32.8 | 1000. | 218.7 |
| 2 | 0.976 | 27.0 | | |
| 3 | 1.000 | 0.0 | -959.1 | 357.6 |
| 4 | 0.938 | 17.9 | | |

Bus Data for 500 MW Transfer Under Line Outage Condition

| Bus | $|V|$ pu | $\theta$ degrees | $P_{gen}$ MW | $Q_{gen}$ Mvar |
|---|---|---|---|---|
| 1 | 1.000 | 29.6 | 500. | 94.6 |
| 2 | 0.988 | 26.7 | | |
| 3 | 1.000 | 0.0 | -481.6 | 164.3 |
| 4 | 0.947 | 17.8 | | |

Generator Data

| H = 5.00 | $X'_d$ = 0.30 | $T'_{do}$ = 7.50 |
|---|---|---|
| $X_d$ = 1.00 | $X''_d$ = 0.25 | $T''_{do}$ = 0.09 |
| $X_q$ = 0.70 | $X''_q$ = 0.25 | $T''_{qo}$ = 0.20 |

Reactances are given in per unit; time constants and inertia in seconds.

A.2 Generator Model

The fifth-order model for the synchronous generator is described by the standard equations, with generator saturation effects ignored for the analysis presented in this paper. The remaining system data is given along the text of this paper.

The generator excitation control, for all cases, has the following first order transfer function.

$$AVR(s) = \frac{75}{1 + s\,0.05}$$